ACS OMEGA

Open Access

http://pubs.acs.org/journal/acsodf

Article

Ammonia Sensing Performance at Room Temperature of Ca-Doped CNFs/Al_2O_3 Gas Sensor

He Gong, Lingyun Ni, Hongli Chao, Zeye Liu, Hang Zhu, Tianli Hu, Ying Guo, Zhiqiang Cheng, Ye Mu,* and Daming Zhang*

Cite This: *ACS Omega* 2024, 9, 42932−42943

ABSTRACT: When NH_3 in the environment exceeds a certain concentration, it may have adverse effects on human health. Ammonia gas sensors currently on the market usually work under high temperatures and are not only expensive but also have poor performance in terms of selectivity. Therefore, the preparation of an ammonia gas sensor that works at room temperature, is low cost, and has high sensitivity and selectivity is particularly important. This paper introduces a room temperature ammonia gas sensor based on a Ca-doped CNFs/Al_2O_3 nanocomposite material, prepared using electrospinning, pre-oxidation, and carbonization processes. The surface morphology, microstructure, and chemical composition of the materials have been characterized by scanning electron microscopy, Raman, and X-ray photoelectron spectroscopy. The Ca-doped CNFs/Al_2O_3 gas sensor has excellent selectivity for ammonia at room temperature and low sensitivity to other volatile gases such as ethanol, dimethylformamide, HCl, and methanol. At 100 ppm of NH_3, the response value of the Ca-doped CNFs/Al_2O_3 gas sensor can reach 22.73, demonstrating excellent repeatability and long-term stability. Its performance is not affected by environmental temperature and humidity, providing great convenience for practical applications. In addition, we also discuss the sensing mechanism of the Ca-doped CNFs/Al_2O_3 gas sensor. This paper not only provides effective materials and methods for the development of high-performance room temperature ammonia gas sensors but is also expected to play a role in the field of environmental monitoring.

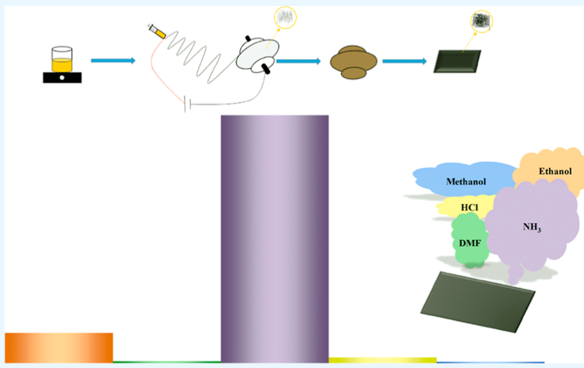

1. INTRODUCTION

With the development of industry and the improvement of people's living standards, the problem of air quality has attracted more and more attention. As a common poisonous gas pollutant, when the ammonia concentration in the environment is too high, it will affect people's health. The United States Occupational Safety and Health Administration issued the standard (29 CFR 1910.1000), stating that the human acceptable concentration limit of ammonia is 25×10^{-6} (not more than 8 h). When the concentration exceeds 500×10^{-6}, it can cause lung damage and even death.[1,2] Therefore, it is very important to realize the quantitative detection of ammonia gas through reliable gas sensors. The common ammonia detection methods have some problems, such as high cost, nonreal-time monitoring, and difficulty in being widely used. With the development of materials and preparation processes, flexible electronics gradually play a huge advantage in the medical and health fields and also play an important role in the industrial field of real-time monitoring and leakage alarms of gases. Metal oxide semiconductor (MOS) materials, polyaniline (PANI) conductive polymer materials, and their composites are commonly used as ammonia-sensitive materials, but these sensors generally have problems with high operating temperatures and poor selectivity. Zou[3] prepared the $Fe_2(MoO_4)_3$/MXene composite material, which operates at a lower temperature (160 °C), has fast response/recovery times (18/24 s), and demonstrates outstanding reversibility as well as long-term stability. Yang[4] prepared $NiWO_4$ materials through a simple coprecipitation method and then added multiwalled carbon nanotubes (MWCNTs) to prepare $NiWO_4$/MWCNTs ammonia gas sensing material, the response/recovery time at 460 °C reached 53/177 s.

By changing the surface morphology of the gas sensitive material or doping other elements, the performance of the gas sensitive material can be optimized. Doping not only affects the conductivity and physical and chemical properties of the material[5,6] but also causes oxide semiconductors to produce

Received: June 21, 2024
Revised: September 25, 2024
Accepted: October 1, 2024
Published: October 10, 2024

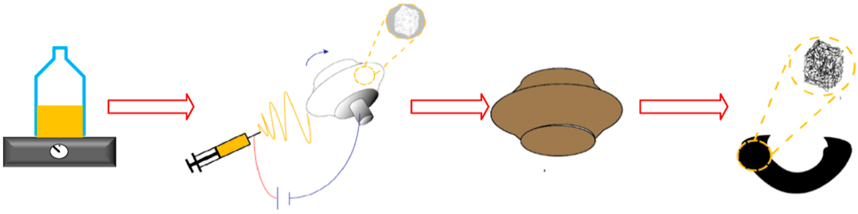

Figure 1. Material preparation process: solution preparation, electrospinning, pre-oxidation, and carbonization.

oxygen vacancies or surface defects, providing more adsorption sites and reaction sites on the surface of the sensing material, thus promoting the surface sensing reaction of the material.[7] Metal doping is one of the most commonly used optimization methods to improve gas sensitivity. In addition to metal doping to optimize the performance of gas sensors, many methods such as morphology and structure regulation, nonmetallic doping to construct heterojunctions, and the introduction of carbon-based nanomaterials have been put into practical work, forming a variety of excellent selectivity gas sensors. Zhang[8] used Pt-modified NB-doped TiO_2 nanosheets as sensing material to prepare a MEMS hydrogen sensor that works at room temperature. The sensor has the advantages of a small size, low power consumption, easy integration, and excellent sensing performance. Pan[9] used MIL-88 as a template and employed solvothermal and calcination methods to synthesize reduced graphene oxide (rGO)-doped nanooctahedral α-Fe_2O_3 nanomaterials on indium tin oxide conductive glass as a self-supporting NO_2 gas sensor. Compared to pure α-Fe_2O_3, the response of the rGO/α-Fe_2O_3 sensor was improved by more than 8 times.

The composite of different materials is the development direction of contemporary materials. The composite heterogeneous nanomaterials exhibit strong interaction between the tightly packed interfaces, which is conducive to the movement of electrons and the increase of the change in electrical conductivity. MOS is widely used in the field of electrochemistry because of its excellent stability, good electrical conductivity, high mechanical strength, wide working range, and low production process. In addition, many metal oxides are good wide-gap N-type semiconductor materials, among which alumina is the most common material. Carbon nanomaterials can significantly improve the electrical conductivity of sensitive materials and provide active sites (oxygen vacancies and defects) for gas adsorption.[10,11] Graphite-ordered carbon nanofibers are P-type semiconductors. The construction of a PN junction leads to the formation of a large number of defect structures on the surface of the material and a large increase in reaction sites and active sites, which is conducive to the analysis and reaction of gas molecules[12,13] and promotes the transfer of carriers, thus generating band bending and internal electric field.

In this paper, CNFs/Al_2O_3 materials were prepared by a simple electrospinning, pre-oxidation, and carbonization method, further doped with alkaline earth metal element-Ca to prepare Ca-doped CNFs/Al_2O_3 materials, characterized the surface morphology, microstructure, and chemical composition, and discussed the gas-sensing mechanism of CNFs/Al_2O_3 composites based on P−N junctions and Ca-doped to improve the sensitivity of the sensors.

2. EXPERIMENTAL SECTION

2.1. Preparation of Materials. The experimental preparation process is shown in Figure 1, which includes solution preparation, electrospinning, pre-oxidation, and carbonization.

2.1.1. Experimental Materials. Experimental materials and basic parameters are shown in Table 1.

Table 1. Materials and Parameters

name	parameter (%)	manufacturer
PAN	≥99.8	Haosheng new material
DMF	≥99.8	Strong functional chemistry
$AlCl_3$	≥97	Chinese experimental material
$CaCl_2$	≥97	Chinese experimental material

2.1.2. Solution Preparation. The solution preparation diagram is shown in Figure 2. Two solutions were prepared. First, 1.2 g of polyacrylonitrile (PAN) was weighed and added to 8.8 g of dimethylformamide (DMF), and the mixture was stirred at 60 °C and 150 rad/min for 4 h in the water bath magnetic stirrer until a uniform solution was obtained. 0.3 g of $AlCl_3$ was added to the one uniform solution, and 0.15 g of $AlCl_3$ and 0.15 g of $CaCl_2$ were added to the other uniform solution. The solutions were stirred at 60 °C and 150 rad/min for 6 h in the water bath magnetic stirrer. After the solutions were well mixed, they were left to stand for 24 h to degas and obtain the spinning solution.

2.1.3. Electrostatic Spinning. The electrostatic spinning unit consists of an electrostatic high-voltage power supply, a solution propulsion unit, a jet port, and a receiving roller, as shown in Figure 3. A kilovolt electrostatic field is applied between the jet and receiver device, and the spinning solution is subjected to the electric field to form a Taylor cone. When the electric field reaches a certain value, a jet is formed from the surface of the droplet to the next region. The jet is dispersed due to the effect of mutual repulsion, forming a large number of fibers. Finally, nanofilm materials can be obtained on the receiving device.[14−16]

At a temperature of 20 °C and a relative humidity of 40%, the spinning solution was added into the syringe, and the receiving roller was 180 mm away from the syringe needle. The positive electrode of the high-voltage power supply was connected to the needle of the syringe, and the negative electrode was connected to the receiving roller. The spinning voltage was set to 15 kV, the solution advancing speed was 0.5 mL/h, and the speed of the steel roller was limited to 120 rad/min. After electrostatic spinning, white nanomembrane materials were obtained.

2.1.4. Pre-Oxidation. The material was put into the air circulation oven, the temperature was set to 60 °C, and the time was set to 3 h for initial oxidation. The white nanofibrous material turned light yellow. The air circulation oven

https://doi.org/10.1021/acsomega.4c05814
ACS Omega 2024, 9, 42932−42943

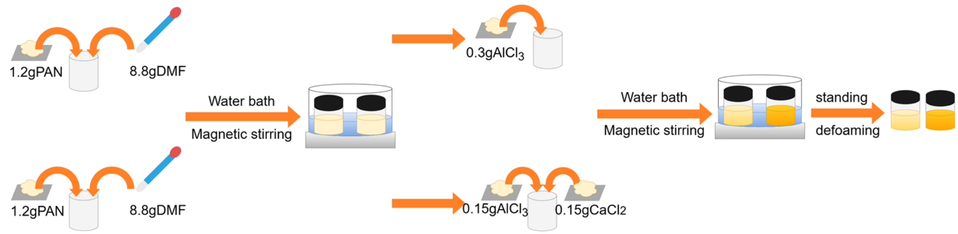

Figure 2. Schematic diagram of solution preparation.

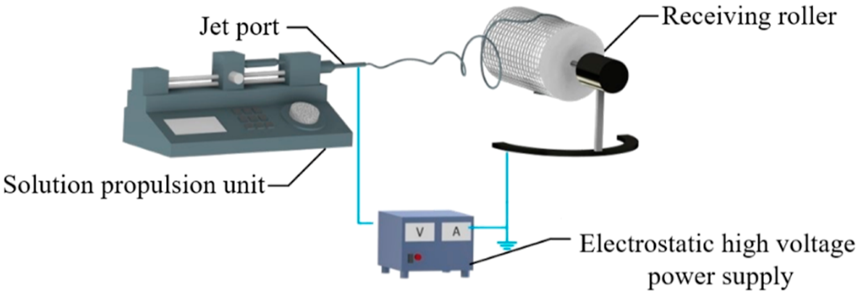

Figure 3. Electrostatic spinning device.

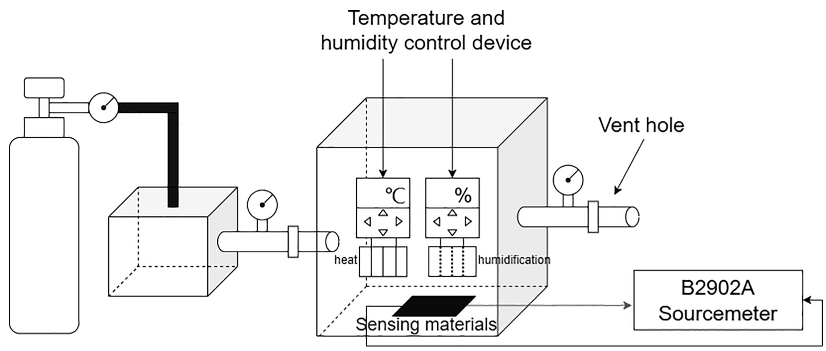

Figure 4. Schematic diagram of the gas-sensitive test device.

temperature was adjusted to 200 °C, and the time was adjusted to 2 h for further oxidation, the nanofibrous material will appear tan. Allow the material to cool naturally to complete the pre-oxidation.

2.1.5. Carbonization. The material was put into the tube furnace; the control atmosphere was nitrogen; the heating rate was 5 °C/min; and the temperature was heated to 1050 °C for 1 h. The nanofibers gradually change from earthen yellow to black, completing the carbonization, and obtain CNFs/Al_2O_3 and Ca-doped CNFs/Al_2O_3 materials.

2.2. Fabrication and Measurement of the Gas Sensors. Separately cut the CNF/Al_2O_3 compound and Ca-doped CNF/Al_2O_3 compound into uniform shapes measuring 2 × 1 cm each, then attached copper foil to both ends of the samples using conductive gel. Ammonia gas sensors based on CNF/Al_2O_3 and Ca-doped CNF/Al_2O_3 were fabricated.

The gas-sensitive environment adopts a straight-through method and uses a thick, airtight component box. The interior is equipped with a temperature and humidity control device, with the ambient temperature set to range between 20 and 25 °C and the humidity set between 20 and 30%. Place the prepared sensor in the component box, connect the test electrode to the digital source meter B2902A, and set the voltage to 2 V. The initial resistance of the prepared sensor is about 2.75 kΩ at room temperature, and heat will be generated on the resistor R when the voltage V is applied. The power P is given by the formula: $P = V$^2/R and the result is 1.5 mW. In this case, the heat generated is small and will not cause a temperature rise. The inlet of the component box is connected to the NH_3 cylinders, and the outlet of the component box is connected to waste gas treatment equipment. Measure the resistance of the material under different NH_3 concentration changes. The schematic diagram of the gas-sensitive test device is shown in Figure 4.

3. RESULTS AND DISCUSSION

3.1. Material Characterization. The material scanning electron microscopy (SEM) is shown in Figure 5, and the fiber

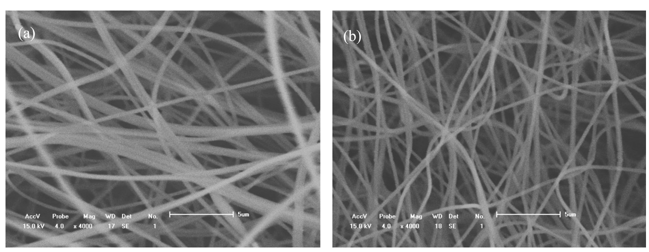

Figure 5. SEM image of materials: (a) CNFs/Al_2O_3 materials and (b) Ca-doped CNFs/Al_2O_3 materials.

https://doi.org/10.1021/acsomega.4c05814
ACS Omega 2024, 9, 42932−42943

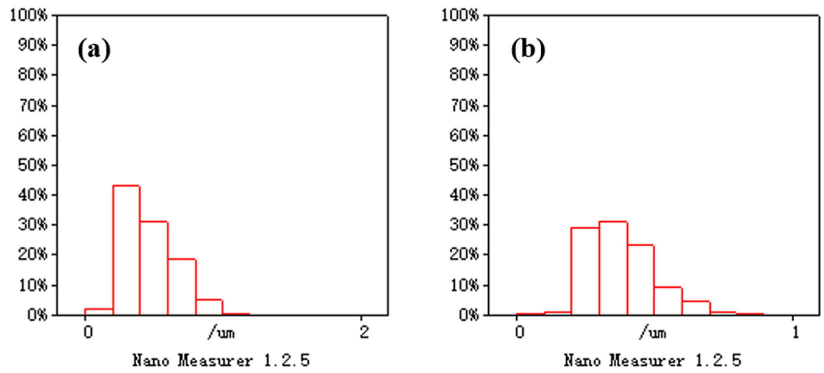

Figure 6. Fiber diameter square diagram: (a) CNFs/Al_2O_3 nanometer fiber and (b) Ca-doped CNFs/Al_2O_3 nanometer fiber.

diameter square is shown in Figure 6. Under a magnification of 5 μm, the average diameter of CNFs/Al_2O_3 nanofiber material (a) is 460 nm, and the average diameter of Ca-doped CNFs/Al_2O_3 nanofiber material (b) is 390 nm. The fibers are stacked fluffy and relatively uniform, and the fiber diameter uniformity is high. Also, the surface is relatively smooth, indicating that the material barrier is small, which is conducive to the material carrier transport.

By observation of the surface morphology of the material through SEM, representative areas were selected for energy-dispersive system (EDS) analysis. By bombarding the sample surface with a high-energy electron beam, we excited characteristic X-rays of different elements. These X-rays were then analyzed for energy using an energy dispersive spectrometer to determine the types and content of elements in the material, as shown in Figure 7. CNFs/Al_2O_3 nanofiber materials (a) mainly contain C, O, and Al elements, of which C element content is the largest, accounting for 35%, Al element 20%, and O element 10%. Ca-doped CNFs/Al_2O_3 nanofiber material (b) mainly contains C, O, Al, Ca, and Cl elements, of which C element has the highest content, accounting for 31%, Al element 14%, Ca element 11%, O element 9%, and Cl element 8%.

As shown in Figure 8, for the carbonization of CNFs/Al_2O_3 material and Ca-doped material, the effect of the degree of graphitization was studied by Raman spectroscopy. The Raman characteristic peaks of C atom crystals of the two materials have two characteristic peaks belonging to the D band and G band at about 1340 and 1580 cm^{-1}. The D-band originates from the lattice edge defects of the undirected carbon, whereas the G-band is the in-plane telescopic vibration of the C-atoms with sp^2 hybridization related to the lattice of the ideally graphitized carbon. The calculated integral plane of D and G bands shows that the I_D/I_G value of the CNFs/Al_2O_3 material is 1.22, and the I_D/I_G value of the Ca-doped CNFs/Al_2O_3 material is 1.51. This indicates that the Ca-doped CNFs/Al_2O_3 material has more defects in the C atomic lattice than the CNFs/Al_2O_3 material, and the defects of the C atomic lattice may increase the surface active sites of the material, which can serve as the adsorption sites of gas molecules. More active sites may mean a higher gas adsorption capacity and thus improved gas sensitivity.

Through X-ray photoelectron spectroscopy (XPS) testing of CNFs/Al_2O_3 materials, as shown in Figure 9, it is known that the material mainly contains three elements: C, O, and Al. Next, analyzing the detailed spectrum of carbon elements reveals that the main carbon functional groups in the material include C−C (284.8 eV), C−O (286.67 eV), and C═O (288.61 eV), with corresponding contents of 69.7, 18.78, and 11.5 at %, respectively. Regarding the oxygen element, convolution analysis indicates that oxygen in the material mainly exists in the forms of Al_2O_3 (531.3 eV), C═O (532.61 eV), and C−O (533.92 eV), with Al_2O_3 content at 17.47 at %, C═O functional group content at 72.59 at %, and C−O functional group content at 9.94 at %. Furthermore, detailed spectrum analysis of Al elements shows the presence of material signal peaks for Al_4C_3 (73.13 eV) and Al_2O_3 (74.18 eV), with respective contents of 35.55% and 64.45 at %, consistent with the results of oxygen element spectrum analysis. In conclusion, it is evident that Al_2O_3 and Al_4C_3 substances are formed in the material.

As shown in Figure 10, further research on the elemental composition and existing forms of elements in Ca-doped CNFs/Al_2O_3 materials is conducted through XPS testing. Characterization of the material through XPS testing revealed that the material mainly consisted of four elements: C, O, Al, and Ca. Analysis of the fine spectrum of carbon elements in the material showed that carbon functional groups mainly included C−C (284.8 eV, 68.54 at %), C−O (286.14 eV, 24.09 at %), and C═O (289.08 eV, 7.37 at %). Convolution analysis of the fine oxygen spectrum indicated the presence of oxygen elements in the material primarily in the forms of CaO (529.87 eV), Al_2O_3 (531.25 eV), C═O (532.53 eV), and C−O (533.82 eV), with contents of 5.58, 44.84, 40.33, and 9.25 at %, respectively. Further analysis of the fine aluminum spectrum revealed the existence of Al elements in the material in the form of Al_4C_3 (73.1 eV) and Al_2O_3 (74.37 eV), with contents of 40.64 and 59.36 at %, respectively. Lastly, analysis of the fine calcium spectrum indicated the presence of four peaks for Ca elements, with peaks at 346.82 and 350.32 eV attributed to the associated spectra CaC_2 2p$_{3/2}$ and CaC_2 2p$_{1/2}$ of CaC_2, while the other two peaks belonged to the characteristic peaks of CaO 2p$_{3/2}$ (347.86 eV) and CaO 2p$_{1/2}$ (351.17 eV). Convolution analysis revealed a CaC_2 content of 42.43 at % and a CaO content of 57.57 at %, consistent with the fine oxygen spectrum analysis results. In conclusion, it can be inferred that Al_2O_3, Al_4C_3, CaC_2, and CaO are generated in Ca-doped CNFs/Al_2O_3 materials.

3.2. Gas Sensing Properties. Figure 11a,b shows the resistance changes of the CNFs/Al_2O_3 gas sensor and Ca-doped CNFs/Al_2O_3 gas sensor when exposed to different concentrations of NH_3 at room temperature, ranging from 0 to 200 ppm. It can be observed that the CNFs/Al_2O_3 gas sensor and the Ca-doped CNFs/Al_2O_3 gas sensor exhibit a rapid rise in resistance when exposed to NH_3 and can recover to their initial values in air. Figure 11c,d shows the resistance change

https://doi.org/10.1021/acsomega.4c05814
ACS Omega 2024, 9, 42932−42943

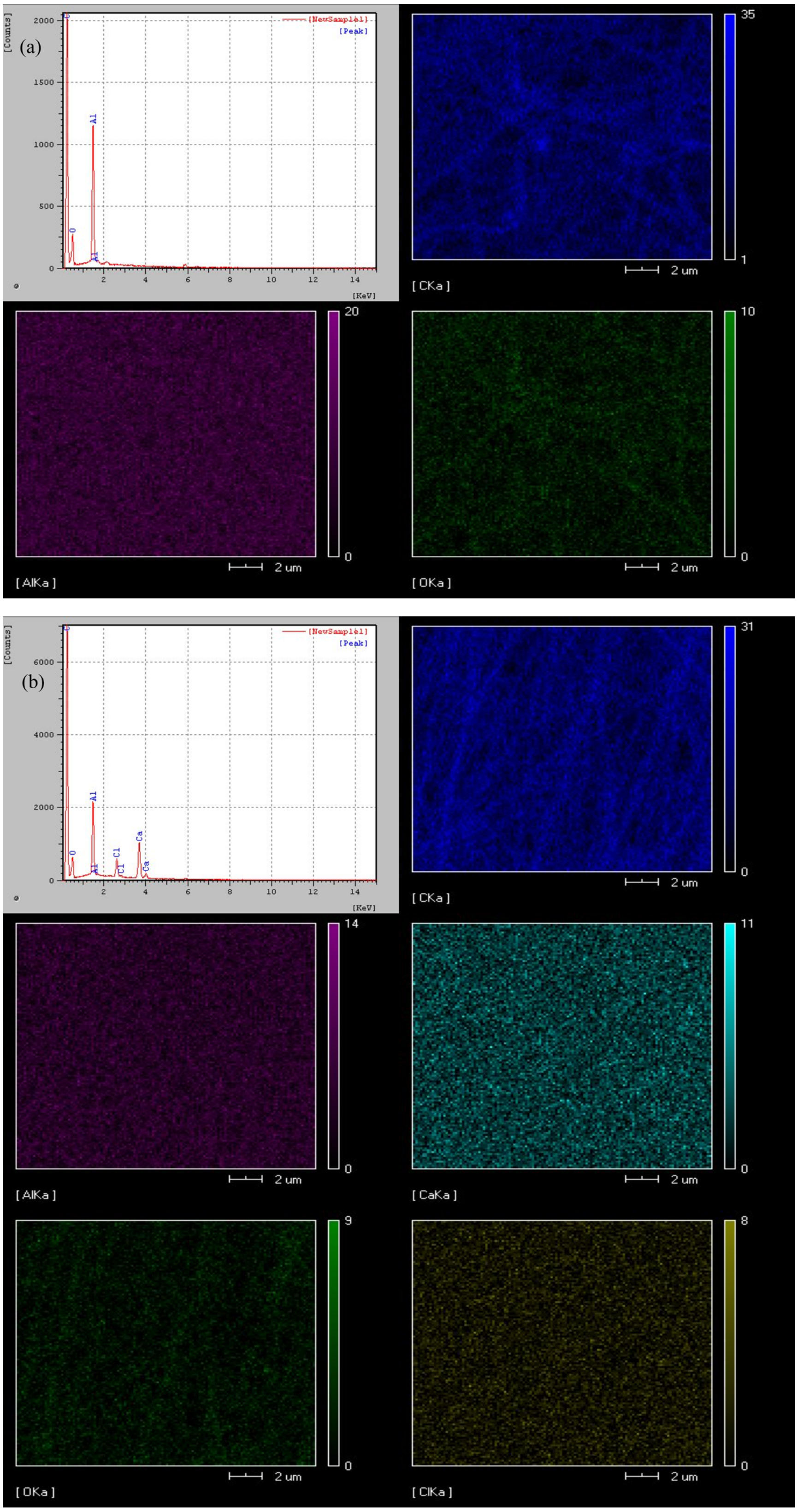

Figure 7. EDS image of materials: (a) CNFs/Al_2O_3 materials and (b) Ca-CNFs/Al_2O_3 materials.

rate of the CNFs/Al_2O_3 gas sensor and the Ca-doped CNFs/Al_2O_3 gas sensor within the range of 0−200 ppm ammonia concentration, and it can be seen that they both have a good linear relationship. However, the Ca-doped CNFs/Al_2O_3 gas sensor has a higher response value in the range of 0 to 200 ppm of NH_3.

To assess the selectivity of the Ca-doped CNFs/Al_2O_3 gas sensor, tests were conducted using various gases, including

https://doi.org/10.1021/acsomega.4c05814
ACS Omega 2024, 9, 42932−42943

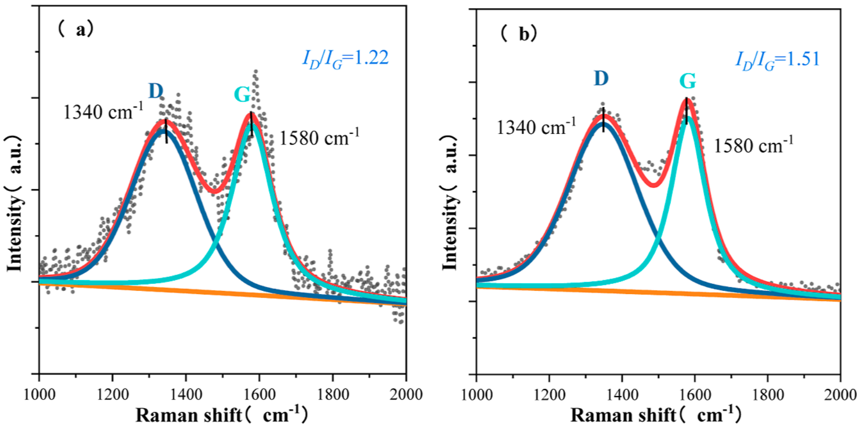

Figure 8. Raman spectra of materials: (a) CNFs/Al_2O_3 materials and (b) Ca-doped CNFs/Al_2O_3 materials.

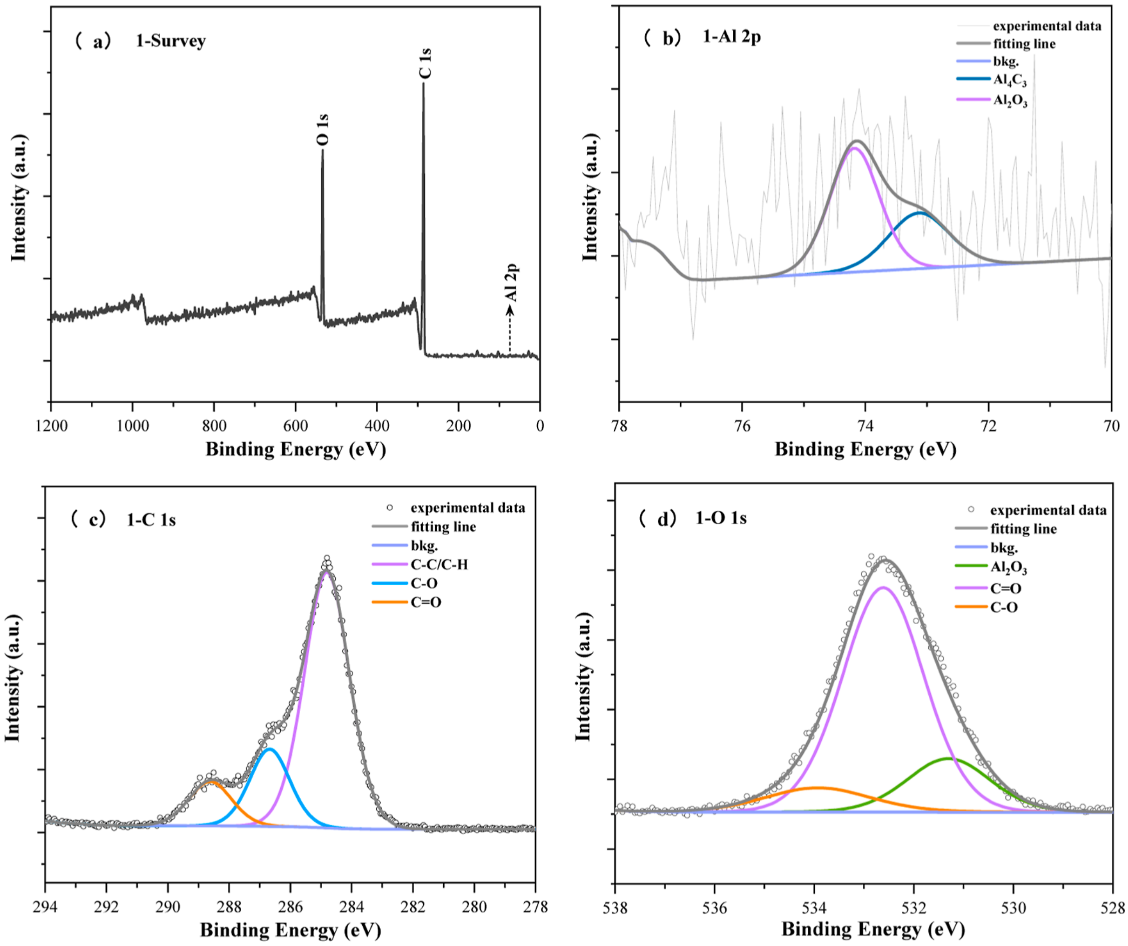

Figure 9. XPS characterization of CNFs/Al_2O_3 materials: (a) CNFs/Al_2O_3 materials' survey; (b) Al 2p; (c) C 1s; and (d) O 1s.

ethanol, DMF, NH_3, HCl, and methanol. As shown in Figure 12, the Ca-doped CNFs/Al_2O_3 gas sensor at room temperature has an extremely high selectivity for NH_3, while its sensitivity to several other test gases is relatively low. Because ammonia molecules contain lone pairs of electrons, they can form strong coordination bonds with Ca^{2+}. In contrast, although molecules such as ethanol and methanol also have lone pair electrons, they have a weak affinity with calcium ions; therefore, the Ca-doped CNFs/Al_2O_3 material has better selectivity for NH_3.

Repeatability and response/recovery time are important indicators to measure the self-recovery ability of the sensor. The response time of the gas sensor refers to the time required for the sensor to go from contact with the target gas to the output stability signal, and the recovery time refers to the time required for the sensor to go from the target gas to the output signal to recover to the initial state. The response/recovery time of the gas sensor was tested in a gas-sensitive test environment with a concentration of 0−50 ppm ammonia, and the test was carried out in 5 cycles. As shown in Figure 13, the response/recovery time of the sensor prepared in this paper is 221/226 s, 5 cycles maintain good repeatability. The SEM in Figure 5 shows that the increased porosity of the Ca-doped

https://doi.org/10.1021/acsomega.4c05814
ACS Omega 2024, 9, 42932−42943

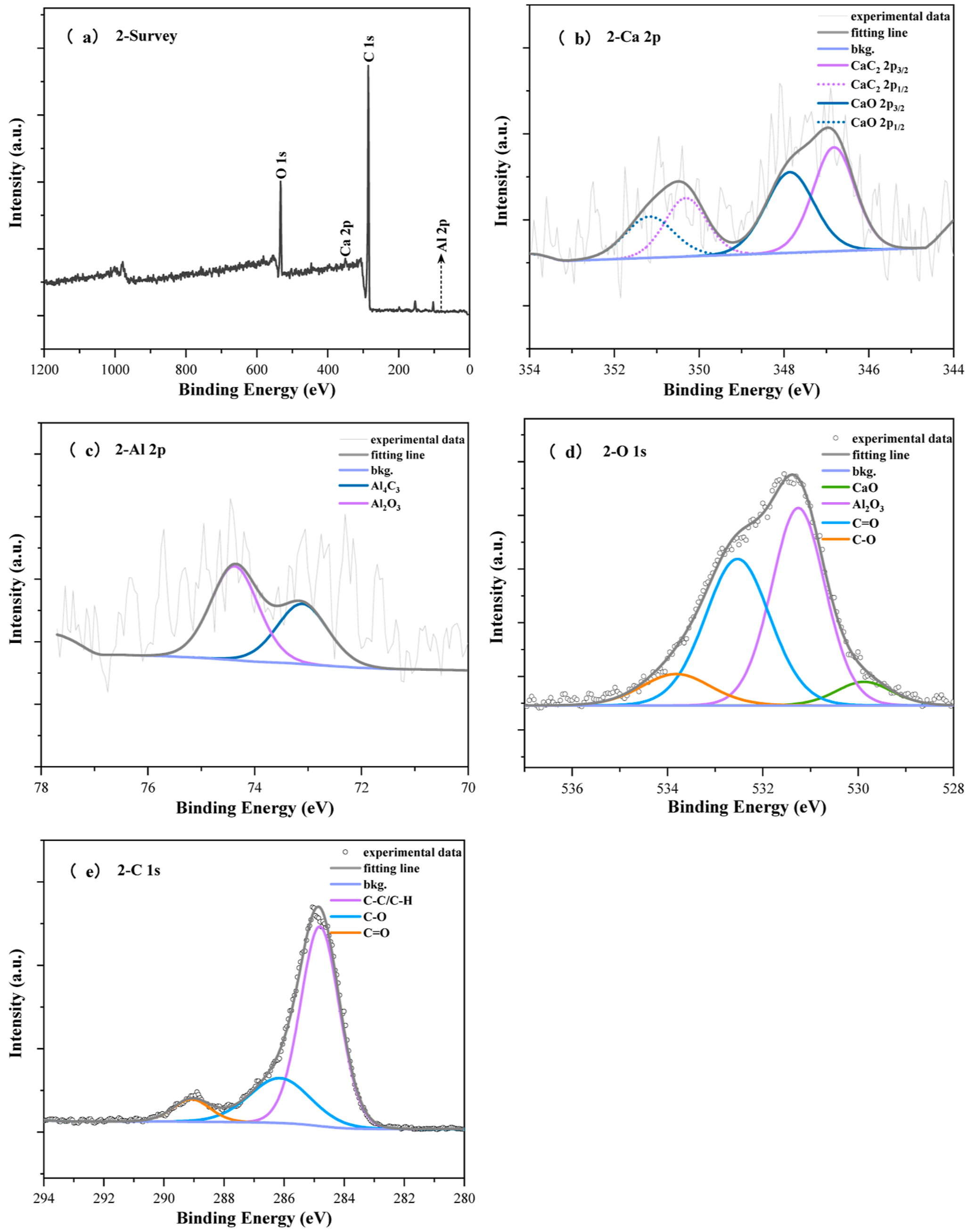

Figure 10. XPS characterization of Ca-doped CNFs/Al_2O_3 materials: (a) Ca-doped CNFs/Al_2O_3 material's survey; (b) Al 2p; (c) Ca 2p; (d) C 1s; and (e) O 1s.

CNFs/Al_2O_3 material can serve as a channel for ammonia molecules to enter and leave the surface of the material, accelerating the adsorption and desorption rate. After repeated cycle testing, the sensor still maintains good response ability and recovery ability, and the peak value of the sensor in the cycle test remains basically unchanged, demonstrating good sensing characteristics and repeatability.

In order to evaluate the long-term stability and service life of the Ca-doped CNFs/Al_2O_3 sensor, the sensor material was placed in a gas sensitive test device containing 50 ppm of NH_3 for 15 days, and the change of the resistance value of the sensor was recorded at a fixed time every day. As shown in Figure 14, the resistance value of the sensor is almost unchanged within 15 days, indicating that the sensor shows good long-term stability.

To test whether Ca-doped CNFs/Al_2O_3 can maintain its NH_3 sensitivity under deformation conditions, the fixing and stretching device of the material is shown in Figure 15a, and the measurement method of bending angle is shown in Figure 15b. The material was bent at 0, 5, 10, 30, 45, and 90° and tested at different ammonia concentrations. As shown in Figure 16, with the increase of the gas concentration, the resistance change rate of materials with different bending degrees is basically the same. The results show that the prepared sensing material has good flexibility, and the deformation does not affect its gas sensitivity. It can be used for ammonia gas monitoring under long-term deformation.

The Ca-doped CNFs/Al_2O_3 material was tested for temperature and humidity. The gas-sensitive test device interior is equipped with a temperature and humidity control

https://doi.org/10.1021/acsomega.4c05814
ACS Omega 2024, 9, 42932−42943

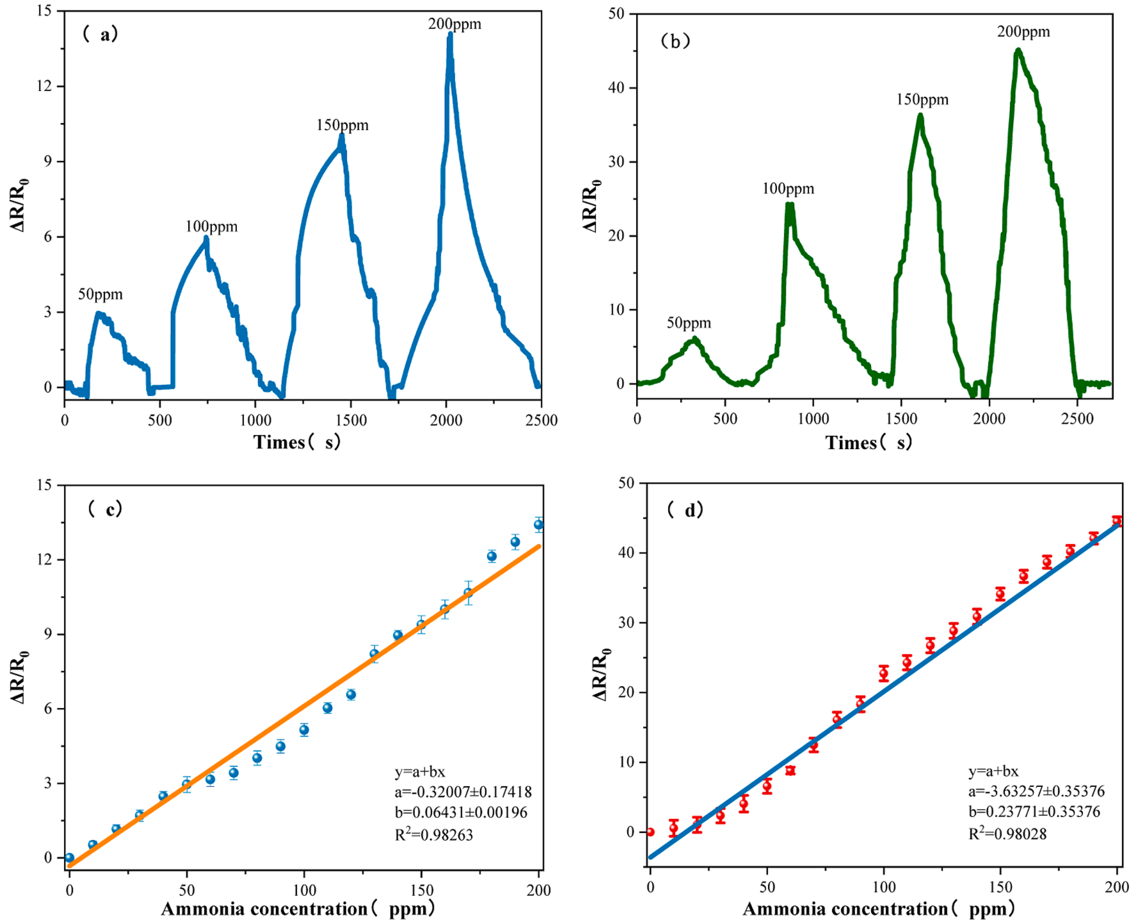

Figure 11. (a) Response of CNFs/Al_2O_3 to different NH_3 concentrations; (b) response of Ca-doped CNFs/Al_2O_3 to different NH_3 concentrations; (c) fitting curve of CNFs/Al_2O_3 in different NH_3 concentrations; and (d) fitting curve of Ca-doped CNFs/Al_2O_3 in different NH_3 concentrations.

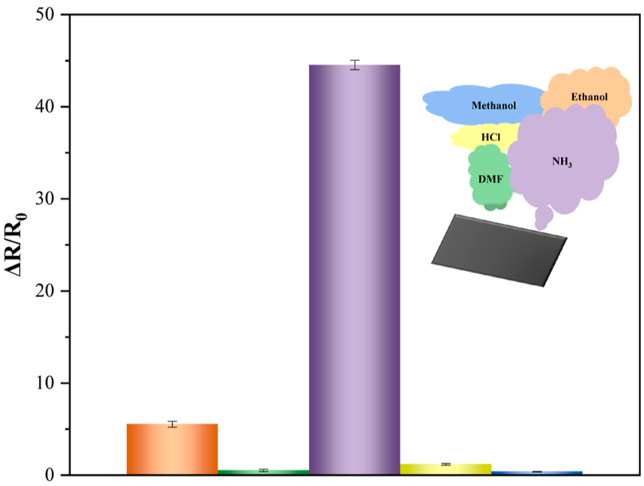

Figure 12. Ca-doped CNFs/Al_2O_3 selectivity test of the gas sensor.

device. For the humidity sensitivity test, the humidity control device was turned on, the humidity range was tested from 20 to 80%, and the resistance value was recorded under different humidity, and the test results are shown in Figure 17a. For the temperature sensitivity test, turn on the temperature control device, test the temperature range of 20∼60 °C, and record the resistance value at different temperatures. The test results are shown in Figure 17b. The test shows that the change of temperature and humidity has little influence on the change rate of resistance, and there is no good linear relationship, which proves that the prepared sensing material is not sensitive to temperature and humidity and has good environmental stability.

As shown in Table 2, a comparison of this study with other reported ammonia sensors indicates that the Ca-doped CNFs/Al_2O_3 gas sensor prepared in this paper is relatively superior to other published ammonia gas sensors.

3.2.1. Gas-Sensing Mechanism. By doping with calcium, the purpose is to introduce additional electrons into the lattice of Al_2O_3. Ca, as a more active divalent cation, may substitute for aluminum atoms and release electrons to the conduction band. The doping process creates lattice defects, such as oxygen vacancies, which can trap electrons. The addition of the alkaline earth metal element Ca increases the oxygen vacancy on the surface of the material. Oxygen molecules in the air are adsorbed on the surface of the semiconductor material, further increasing the adsorption and reaction sites of the material and enhancing the material's trapping and reaction ability to oxygen atoms, thus improving the response to NH_3.

In this article, a high-response sensitive metal oxide is combined with carbon nanofibers by electrospinning technology to obtain a Ca-doped CNFs/Al_2O_3 gas sensor. The synergic effect of carbon nanomaterials and metal oxides is utilized to improve the gas-sensitive performance of the gas sensor. The Ca-doped CNFs/Al_2O_3 gas sensor exhibits P-type

https://doi.org/10.1021/acsomega.4c05814
ACS Omega 2024, 9, 42932−42943

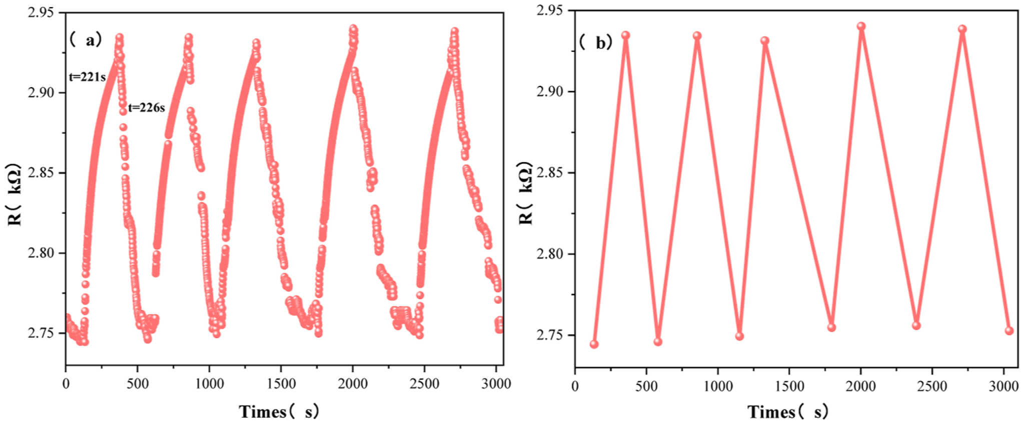

Figure 13. Ca-doped CNFs/Al_2O_3 50 ppm of NH_3 cycle test: (a) dynamic response of Ca-doped CNFs/Al_2O_3 and (b) fitting curve of Ca-doped CNFs/Al_2O_3.

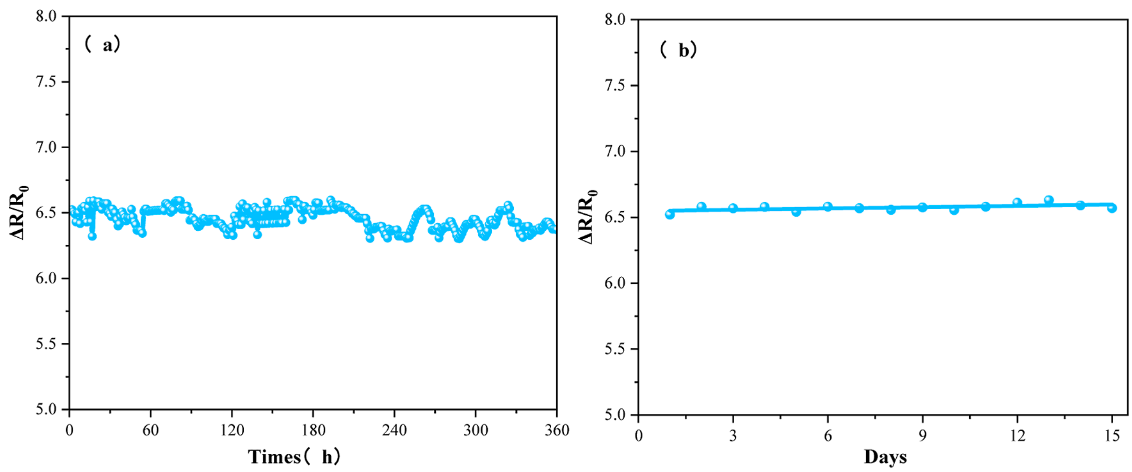

Figure 14. Long-term stability test of Ca-doped CNFs/Al_2O_3: (a) dynamic response of Ca-doped CNFs/Al_2O_3 and (b) fitting curve of Ca-doped CNFs/Al_2O_3.

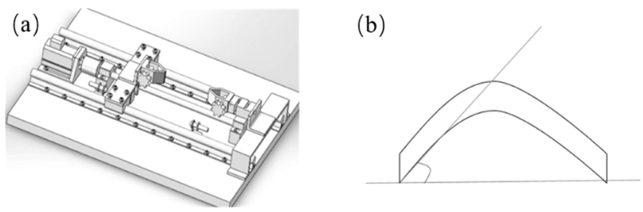

Figure 15. (a) Schematic diagram of a self-made testing machine and (b) measurement diagram of the bending angle.

characteristics, which means that CNFs are dominant. The gas-sensitive properties of the material are mainly achieved by the chemical reaction between the target gas molecules and the oxygen adsorbed on the semiconductor surface. As shown in formulas 1 and 2, the sensing mechanism of the MOS nanostructure (SMON)-based ammonia sensor operating at room temperature is based on the reaction between NH_3 gas molecules and O_2^- adsorbed on the surface of SMON ammonia sensor.[25,26] When SMON's ammonia sensor is in an air environment, the oxygen molecules in the air are easily adsorbed on the surface and will be converted into oxygen ions in the form of atoms or molecules due to their high electron affinity[27,28]

$$NH_{3(gas)} \rightarrow NH_{3(ads)} \tag{1}$$

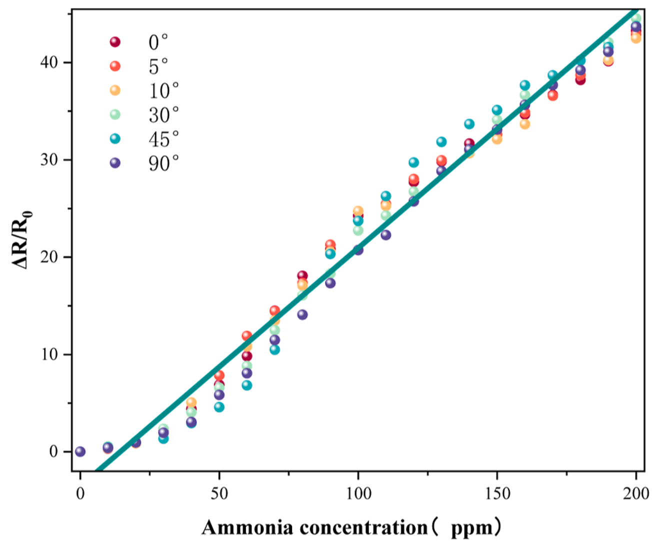

Figure 16. Ca-doped CNFs/Al_2O_3 flexible test under NH_3.

$$4NH_{3(ads)} + 3O_2^- \rightarrow 2N_2 + 6H_2O + 3e^- \tag{2}$$

As an N-type semiconductor, Ca-doped Al_2O_3 is in contact with a graphite-ordered carbon nanofiber (P-type semiconductor) to form a semiconductor PN junction, creating

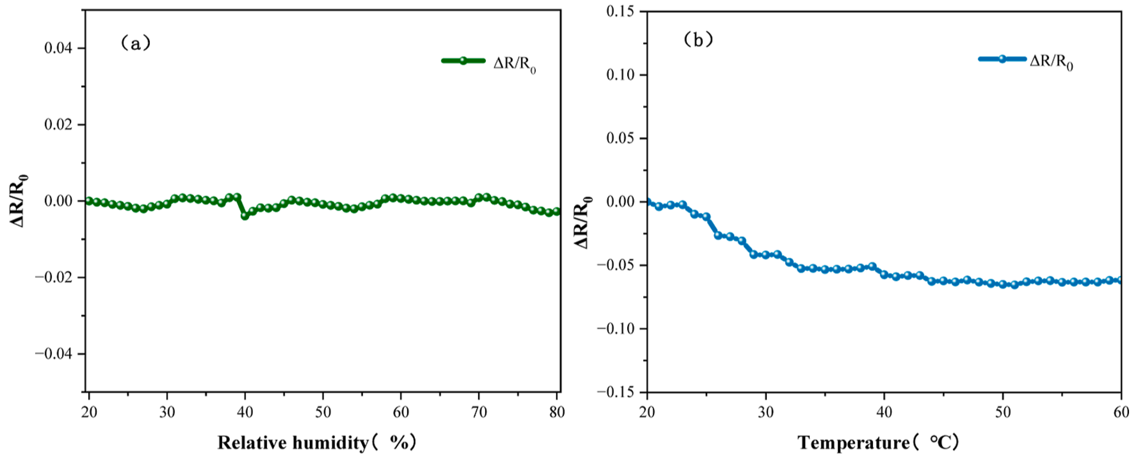

Figure 17. Sensor environmental stability test diagram: (a) humidity stability and (b) temperature stability.

Table 2. Comparison of This Study with Other Reported Ammonia Sensors

materials	target gas	response value	response/recovery time	concentration (ppm)	operating temperature (C°)	references
Pt/WO_3	NH_3	26.9	−/60 min	1000	250	17
ZnO/rGO	NH_3	10.96	153/79 s	100	25	18
Pt/WS_2	NH_3	14.5	200/1200 s	500	25	19
$PANI/MoS_2/SnO_2$	NH_3	10.9	21/130 s	100	RT	20
functionalized SWCNTs	NH_3	5.8	3/7 min	8	40	21
IO/WS_2	NH_3	3.81	88/116 s	10	RT	22
PANI graft film	NH_3	12	7/20 min	50	50 °C	23
PANI-MWCNTs/PDMS	NH_3	12	100/236 s	40	RT	24
Ca-doped CNFs/Al_2O_3	NH_3	22.73	221/226 s	50	RT	this paper

an electron flow at the contact interface. When a Ca-doped CNFs/Al_2O_3 gas sensor is exposed to air at room temperature, Ca-doped Al_2O_3 nanoparticles on the surface of CNFs adsorb oxygen molecules, which react with electrons to produce O_2^-, as shown in formula 3. Sensors based on carbon nanomaterials can ionize adsorbed oxygen into O_2^- ions at room temperature, but O_2^- ions are not sufficient to convert ammonia to N_2 and H_2O at room temperature. At room temperature, when exposed to ammonia, the following reactions occur between ammonia and the adsorbed oxygen ions, O_2^-, as shown in formula 4, and sensing mechanism diagram as shown in Figure 18

$$O_{2(gas)} + e^- \rightarrow O^-_{2(ads)} \quad (3)$$

$$4NH_3 + 5O_2^- \rightarrow 4NO + 6H_2O + 6e^- \quad (4)$$

The contact between an N-type semiconductor and a P-type semiconductor constitutes a semiconductor PN junction, and the construction of the PN junction results in the formation of a large number of defect structures on the surface of the material, significantly increasing reaction sites and active sites, which is conducive to the analysis and reaction of gas molecules.[29] This is the basic principle that the construction of the PN junction can improve the gas-sensitive performance of the sensor. CNFs exhibit P-type semiconductor properties, and Ca-doped Al_2O_3 exhibits N-type semiconductor properties. The two are in close contact at the interface and form PN heterojunctions. As the charge carriers of the two are electrons and holes, respectively, a high-resistance region with a very small number of charge carriers is formed in the Ca-doped CNFs/Al_2O_3 composite at the contact interface due to the combined influence of drift motion and diffusion, which is called the depletion layer.[30] When the material is exposed to ammonia gas, the NH_3 gas molecules combine with the ions on the surface of the material, releasing electrons, which further causes the depletion layer of the PN junction to widen, as shown in Figure 19.

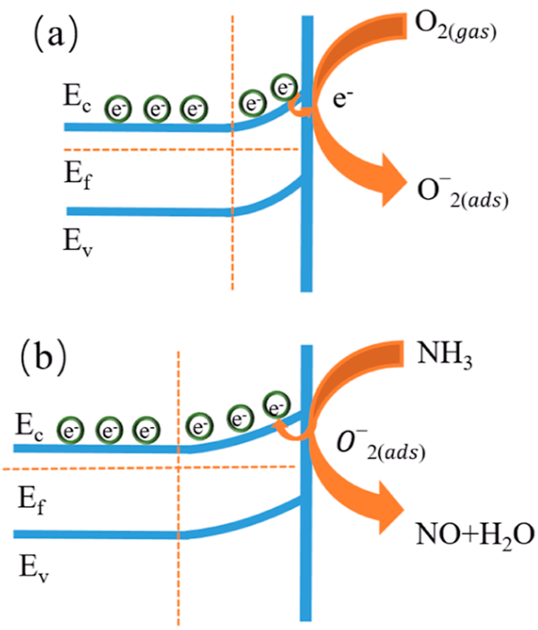

Figure 18. Sensing mechanism diagram: (a) stage I and (b) stage II.

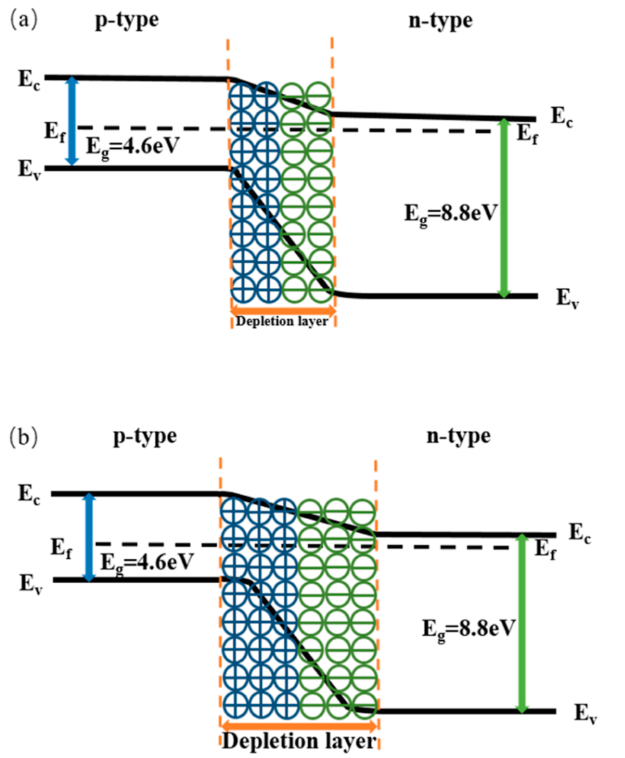

Figure 19. PN junction mechanism diagram: (a) stage I and (b) stage II.

4. CONCLUSIONS

In conclusion, we prepared the CNFs/Al_2O_3 materials using electrospinning, pre-oxidation, and carbonization methods, further doped with alkaline earth metal elements to prepare Ca-doped CNFs/Al_2O_3 materials and characterized the surface morphology, microstructure, and chemical composition of the materials. As can be seen from the gas sensitivity test, the response value of the CNFs/Al_2O_3 gas sensor can reach 5.15 in 100 ppm of NH_3 at room temperature, and the response value of the Ca-doped CNFs/Al_2O_3 gas sensor can reach 22.73 in 100 ppm of NH_3. It can recover the initial value in the air in multiple cycle tests, with good repeatability (5 cycles), and still maintain stable sensing performance in a long-term tests, with good long-term stability (15 days). The Ca-doped CNFs/Al_2O_3 gas sensor has good selectivity for NH_3 at room temperature and is not affected by ambient temperature and humidity in the range of 20−60 °C and 20−80% RH, and can be used for gas monitoring under long-term deformation conditions. The gas-sensitive properties of the Ca-doped CNFs/Al_2O_3 gas sensor are related to key factors, such as the formation of PN junctions and the oxygen adsorption of the material. The observed high response, good NH_3 selectivity, and reproducibility demonstrate that the Ca-doped CNFs/Al_2O_3 material can be used as an NH_3 monitoring material at room temperature.

AUTHOR INFORMATION

Corresponding Authors

Ye Mu − *College of Information Technology, Jilin Agricultural University, Changchun 130118, China; Jilin Province Intelligent Environmental Engineering Research Center, Changchun 130118, China*; Email: muye@jlau.edu.cn

Daming Zhang − *College of Electronic Science and Engineering, Jilin University, Changchun 130012, China*; Email: zhangdm@jlu.edu.cn

Authors

He Gong − *College of Information Technology, Jilin Agricultural University, Changchun 130118, China; College of Electronic Science and Engineering, Jilin University, Changchun 130012, China; Jilin Province Intelligent Environmental Engineering Research Center, Changchun 130118, China*

Lingyun Ni − *College of Information Technology, Jilin Agricultural University, Changchun 130118, China*; orcid.org/0009-0003-1257-0879

Hongli Chao − *College of Information Technology, Jilin Agricultural University, Changchun 130118, China*

Zeye Liu − *College of Information Technology, Jilin Agricultural University, Changchun 130118, China*

Hang Zhu − *College of Information Technology, Jilin Agricultural University, Changchun 130118, China*

Tianli Hu − *College of Information Technology, Jilin Agricultural University, Changchun 130118, China; Jilin Province Intelligent Environmental Engineering Research Center, Changchun 130118, China*

Ying Guo − *College of Information Technology, Jilin Agricultural University, Changchun 130118, China; Jilin Province Intelligent Environmental Engineering Research Center, Changchun 130118, China*

Zhiqiang Cheng − *College of Resources and Environment, Jilin Agricultural University, Changchun 130118, China*; orcid.org/0000-0003-1156-0540

Complete contact information is available at: https://pubs.acs.org/10.1021/acsomega.4c05814

Author Contributions

The manuscript was written through the contributions of all authors. All authors have given their approval to the final version of the manuscript.

Notes

The authors declare no competing financial interest.

ACKNOWLEDGMENTS

This research was funded by the Jilin Provincial Science and Technology Department-Jilin Province germplasm Resources Public Service cloud Platform construction (20210302009NC), the Changchun Science and Technology Bureau-"Research on key technology of Monitoring common pests and insect conditions of main grain Crops based on Internet of Things" project (21ZGN27), and the Jilin Provincial Department of Education-Research on key techniques of individual identification of Sika deer (JJKH20230386KJ).

REFERENCES

(1) Alwarappan, S.; Nesakumar, N.; Sun, D.; Hu, T. Y.; Li, C.-Z. 2D Metal Carbides and Nitrides (MXenes) for Sensors and Biosensors. *Biosens. Bioelectron.* **2022**, *205*, 113943.

(2) Chen, L.; Yu, Q.; Pan, C.; Song, Y.; Dong, H.; Xie, X.; Li, Y.; Liu, J.; Wang, D.; Chen, X. Chemiresistive Gas Sensors Based on Electrospun Semiconductor Metal Oxides: A Review. *Talanta* **2022**, *246*, 123527.

(3) Zou, S.; Gao, J.; Liu, L.; Lin, Z.; Fu, P.; Wang, S.; Chen, Z. Enhanced Gas Sensing Properties at Low Working Temperature of

Iron Molybdate/MXene Composite. *J. Alloys Compd.* **2020**, *817*, 152785.
(4) Yang, M.; Au, C.; Deng, G.; Mathur, S.; Huang, Q.; Luo, X.; Xie, G.; Tai, H.; Jiang, Y.; Chen, C.; Cui, Z.; Liu, X.; He, C.; Su, Y.; Chen, J. $NiWO_4$ Microflowers on Multi-Walled Carbon Nanotubes for High-Performance NH_3 Detection. *ACS Appl. Mater. Interfaces* **2021**, *13* (44), 52850−52860.
(5) Jayasaranya, N.; Pavai, R. E.; Sagadevan, S.; Balu, L.; Manoharan, C. Unveiling of Mn Doped TiO_2 Nanoparticles for Efficient Room Temperature Gas Sensing Performance. *Inorg. Chem. Commun.* **2024**, *162*, 112168.
(6) Xia, L.; Sun, Z.; Wu, Y.; Yu, X.-F.; Cheng, J.; Zhang, K.; Sarina, S.; Zhu, H.-Y.; Weerathunga, H.; Zhang, L.; Xia, J.; Yu, J.; Yang, X. Leveraging Doping and Defect Engineering to Modulate Exciton Dissociation in Graphitic Carbon Nitride for Photocatalytic Elimination of Marine Oil Spill. *Chem. Eng. J.* **2022**, *439*, 135668.
(7) Guo, H.; Yang, C.-Y.; Zhang, X.; Motta, A.; Feng, K.; Xia, Y.; Shi, Y.; Wu, Z.; Yang, K.; Chen, J.; Liao, Q.; Tang, Y.; Sun, H.; Woo, H. Y.; Fabiano, S.; Facchetti, A. F.; Guo, X. Transition Metal-Catalysed Molecular n-Doping of Organic Semiconductors. *Nature* **2021**, *599*, 67−73.
(8) Zhang, M.; He, Z.; Cheng, W.; Li, X.; Zan, X.; Bao, Y.; Gu, H.; Homewood, K.; Gao, Y.; Zhang, S.; Wang, Z.; Lei, M.; Xia, X. A Room-Temperature MEMS Hydrogen Sensor for Lithium Ion Battery Gas Detecting Based on Pt-Modified Nb Doped TiO_2 Nanosheets. *Int. J. Hydrogen Energy* **2024**, *74*, 307−315.
(9) Pan, Z.; Wang, D.; Zhang, D.; Yang, Y.; Yu, H.; Wang, T.; Dong, X. RGO Doped MOFs Derived α-Fe_2O_3 Nanomaterials for Self-Supporting Ppb-Level NO_2 Gas Sensor. *Sens. Actuators, B* **2024**, *405*, 135378.
(10) Liu, S.; Sun, W. Attention Mechanism-Aided Data- and Knowledge-Driven Soft Sensors for Predicting Blast Furnace Gas Generation. *Energy* **2023**, *262*, 125498.
(11) Huang, X.; Pang, R.; Yang, M.; Zhang, S.; Guo, F.; Xu, J.; Zhang, Y.; Cao, A.; Shang, Y. Flexible Gas Sensors Based on Carbon Nanotube Hybrid Films: A Review. *Adv. Mater. Technol.* **2023**, *8*, 2300616.
(12) Zeng, T.; Ma, D.; Gui, Y. Gas-Sensitive Performance Study of Metal (Au, Pd, Pt)/ZnO Heterojunction Gas Sensors for Dissolved Gases in Transformer Oil. *Langmuir* **2024**, *40* (18), 9819−9830.
(13) Yue, Q.; Liu, T.; Mu, Y.; Chen, X.; Yin, X.-T. Highly Responsive and Swift Recovery Triethylamine Gas Sensor Based on $NiCo_2O_4$-ZnO p-n Heterojunction. *Sens. Actuators, B* **2024**, *410*, 135666.
(14) Xue, J.; Wu, T.; Dai, Y.; Xia, Y. Electrospinning and Electrospun Nanofibers: Methods, Materials, and Applications. *Chem. Rev.* **2019**, *119* (8), 5298−5415.
(15) Ghosal, K.; Agatemor, C.; Špitálsky, Z.; Thomas, S.; Kny, E. Electrospinning Tissue Engineering and Wound Dressing Scaffolds from Polymer-Titanium Dioxide Nanocomposites. *Chem. Eng. J.* **2019**, *358*, 1262−1278.
(16) Li, Y.; Wang, S.; Xiao, Z.-C.; Yang, Y.; Deng, B.-W.; Yin, B.; Ke, K.; Yang, M.-B. Flexible TPU strain sensors with tunable sensitivity and stretchability by coupling AgNWs with rGO. *J. Mater. Chem. C Mater.* **2020**, *8*, 4040−4048.
(17) Liu, I.-P.; Chang, C.-H.; Chou, T. C.; Lin, K.-W. Ammonia Sensing Performance of a Platinum Nanoparticle-Decorated Tungsten Trioxide Gas Sensor. *Sens. Actuators, B* **2019**, *291*, 148−154.
(18) Won, M.; Sim, J.; Oh, G.; Jung, M.; Mantry, S. P.; Kim, D. Fabrication of a Fully Printed Ammonia Gas Sensor Based on ZnO/RGO Using Ultraviolet-Ozone Treatment. *Sensors* **2024**, *24* (5), 1691.
(19) Ouyang, C.; Chen, Y.; Qin, Z.; Zeng, D.; Zhang, J.; Wang, H.; Xie, C. Two-Dimensional WS_2-Based Nanosheets Modified by Pt Quantum Dots for Enhanced Room-Temperature NH_3 Sensing Properties. *Appl. Surf. Sci.* **2018**, *455*, 45−52.
(20) Liu, A.; Lv, S.; Jiang, L.; Liu, F.; Zhao, L.; Wang, J.; Hu, X.; Yang, Z.; He, J.; Wang, C.; Yan, X.; Sun, P.; Shimanoe, K.; Lu, G. The Gas Sensor Utilizing Polyaniline/ MoS_2 Nanosheets/ SnO_2 Nanotubes for the Room Temperature Detection of Ammonia. *Sens. Actuators, B* **2021**, *332*, 129444.
(21) Ansari, N.; Lone, M.; Ali, D. J.; Husain, M.; Husain, S. Enhancement of Gas Sensor Response Characteristics of Functionalized SWCNTs. *AIP Conference Proceedings*; AIP Publishing, 2020; Vol. *2276*, p 20033.
(22) Guang, Q.; Huang, B.; Yu, J.; Zhang, J.; Li, X. Indium Oxide Decorated WS_2 Microflakes for Selective Ammonia Sensors at Room Temperature. *Chemosensors* **2022**, *10* (10), 402.
(23) Matsuguchi, M.; Horio, K.; Uchida, A.; Kakunaka, R.; Shiba, S. A Flexible Ammonia Gas Sensor Based on a Grafted Polyaniline Grown on a Polyethylene Terephthalate Film. *Sensors* **2024**, *24*, 3695.
(24) Zhu, C.; Zhou, T.; Xia, H.; Zhang, T. Flexible Room-Temperature Ammonia Gas Sensors Based on PANI-MWCNTs/PDMS Film for Breathing Analysis and Food Safety. *Nanomaterials* **2023**, *13* (7), 1158.
(25) Li, Z.; Li, H.; Wu, Z.; Wang, M.; Luo, J.; Torun, H.; Hu, P.; Yang, C.; Grundmann, M.; Liu, X.; Fu, Y. Advances in Designs and Mechanisms of Semiconducting Metal Oxide Nanostructures for High-Precision Gas Sensors Operated at Room Temperature. *Mater. Horiz.* **2019**, *6* (3), 470−506.
(26) Li, Z.; Lin, Z.; Wang, N.; Wang, J.; Liu, W.; Sun, K.; Fu, Y. Q.; Wang, Z. High Precision NH3 Sensing Using Network Nano-Sheet Co_3O_4 Arrays Based Sensor at Room Temperature. *Sens. Actuators, B* **2016**, *235*, 222−231.
(27) Pan, X.; Zhao, X.; Chen, J.; Bermak, A.; Fan, Z. A Fast-Response/Recovery ZnO Hierarchical Nanostructure Based Gas Sensor with Ultra-High Room-Temperature Output Response. *Sens. Actuators, B* **2015**, *206*, 764−771.
(28) Choi, M. S.; Bang, J. H.; Mirzaei, A.; Na, H. G.; Kwon, Y. J.; Kang, S. Y.; Choi, S.-W.; Kim, S. S.; Kim, H. W. Dual Sensitization of MWCNTs by Co-Decoration with p- and n-Type Metal Oxide Nanoparticles. *Sens. Actuators, B* **2018**, *264*, 150−163.
(29) Lee, J. E.; Lim, C. K.; Park, H. J.; Song, H.; Choi, S.-Y.; Lee, D.-S. ZnO−CuO Core-Hollow Cube Nanostructures for Highly Sensitive Acetone Gas Sensors at the ppb Level. *ACS Appl. Mater. Interfaces* **2020**, *12* (31), 35688−35697.
(30) Mathew, M.; Shinde, P.; Samal, R.; Rout, C. A Review on Mechanisms and Recent Developments in P-n Heterojunctions of 2D Materials for Gas Sensing Applications. *J. Mater. Sci.* **2021**, *56*, 9575−9604.

https://doi.org/10.1021/acsomega.4c05814
ACS Omega 2024, 9, 42932−42943